Journal of Nuclear Materials 390–391 (2009) 606–609

Contents lists available at ScienceDirect

Journal of Nuclear Materials

journal homepage: www.elsevier.com/locate/jnucmat

Ion-driven deuterium permeation through tungsten at high temperatures

Yu.M. Gasparyan [a,b,*], A.V. Golubeva [c], M. Mayer [a], A.A. Pisarev [b], J. Roth [a]

[a] Max-Planck-Institut für Plasmaphysik, EURATOM Association, Boltzmanstrasse 2, D-85748 Garching, Germany
[b] Moscow Engineering and Physics Institute, Kashirskoe sh. 31, Moscow 115409, Russia
[c] RRC 'Kurchatov Institute', Ac. Kurchatov sq., 1/1, Moscow RU-123182, Russia

ARTICLE INFO

PACS:
27.10.+h
66.30.−h
52.40.−w

ABSTRACT

The ion-driven permeation (IDP) through 50 μm thick pure tungsten foils was measured in the temperature range of 823–923 K during irradiation by 200 eV/D^+ ion beam with a flux of 10^{17}–10^{18} D/m^{2}s. Gas driven permeation (GDP) from the deuterium background gas was observed as well. Calculations using both the analytical formula for the diffusion limited regime (DLR) and the TMAP 7 code gave good agreement with the experimental data. Defects with a detrapping energy of (2.05 ± 0.15) eV were found to limit the permeation lag time in our experimental conditions.

1. Introduction

Tungsten is planned to be used in ITER as material for divertor baffles and may be at a later stage also for divertor strike points. All plasma facing components will be irradiated by high ion and neutral fluxes of tritium and deuterium. The divertor region will have the highest irradiation fluxe rising the temperature of some parts up to 1270 K [1]. Therefore, investigation of hydrogen isotopes behavior at high temperatures is of importance from the point of view of tritium inventory.

One of the methods to investigate hydrogen behavior in metals is permeation. Ion-driven permeation (IDP) is the technique relevant for plasma facing materials. There are several reports on hydrogen IDP through pure tungsten [2–5] and tungsten coatings [5,6]. All these experiments were made at temperatures below 823 K. This work is devoted to IDP measurements at higher temperatures up to 923 K.

2. Experimental details

The experiments were performed at the PERMEX facility (IPP, Garching), which will be described in details in [7]. The main parts of the facility are: a high current ion source, a magnetic mass-analyzer, a sample unit, a quadrupole mass-spectrometer (QMS), and an ion gun for back surface cleaning by Ar^+ sputtering.

A tungsten foil sealed by two gold O-rings (27 mm in diameter) was used as a sample. Its front side was bombarded by a monoenergetic mass-analysed deuterium ion beam, and the permeation flux from the back side was measured in the registration chamber. Irradiation was performed by 600 eV D_3^+ ions with a flux of 10^{17}–10^{18} D/m^{2}sec decelerated from 3600 eV. The first set of experiments (ex 1–4) was performed with the last diaphragm placed 300 mm in front of the membrane. Further experiments were performed with two additional diaphragms installed closer (30 mm) to the membrane to provide a more homogeneous beam profile and to suppress secondary electrons by the −20 V potential on the last diaphragm (see Fig. 1). The implantation areas were 1.8 cm^2 and 0.5 cm^2 without and with additional diaphragms, respectively. The spot cleaned by the Ar beam on the back side was 3 cm^2 in area.

The sample unit was placed in a furnace. The sample temperature was routinely controlled by a thermocouple mounted inside the furnace, which was calibrated with an uncertainty of ±15 K by a thermocouple welded directly to the sample.

The permeation signal was measured by a quadrupole mass-spectrometer QMG 422 Pfeiffer. Several masses were monitored, including HD, D_2, HDO, and D_2O. The absolute calibration of the D_2 and H_2 permeation rates was made using a set of calibrated leaks. The sensitivity for HD was taken as the average one between H_2 and D_2 sensitivities.

During IDP runs, HDO and D_2O signals in the registration chamber were at the level of the noise, but the signal of HD was comparable with that of D_2, especially at high temperatures and low fluxes.

All samples were cut from the same sheet of a tungsten foil with a thickness of 50 μm and a purity of 99.97%, produced by Plansee AG. They were ultrasonically cleaned in acetone and alcohol and annealed in situ at 900 K for 10 h before experiments to prevent the effect of annealing during the experiment. Experiments without annealing demonstrated intensive formation of HDO and D_2O molecules. The last set of experiments (ex 14) was performed with

* Corresponding author. Address: Max-Planck-Institut für Plasmaphysik, EURATOM Association, Boltzmanstrasse 2, D-85748 Garching, Germany.
E-mail address: yury.gasparyan@ipp.mpg.de (Yu.M. Gasparyan).

0022-3115/$ - see front matter © 2009 Elsevier B.V. All rights reserved.
doi:10.1016/j.jnucmat.2009.01.172

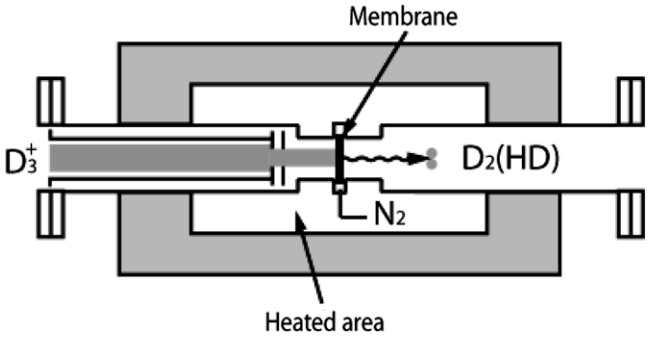

Fig. 1. The scheme of the sample unit.

the sample electrochemically polished from the front side (a middle part with a diameter of 20 mm).

The base pressure during experiments was below 5×10^{-7} Pa (the gauge limit) in the registration chamber and below 10^{-6} Pa in the implantation chamber with hydrogen as the main component. The pressure of D_2 in the implantation chamber during implantation was 7×10^{-4} Pa.

The average grain size observed in SEM was of a few microns in the virgin foil. The thickness of the oxidized layer on the virgin surface estimated by NRA was of a few nanometres.

3. Experimental results

Fig. 2 shows an experimental permeation curve and its comparison with calculations. Calculations were made in two ways: (a) using the TMAP 7 code and (b) applying the simplest analytical formula for GDP in the diffusion limited regime. This formula is well known

$$J(t) = J_0\left[1 + 2\sum_{m=1}^{\infty}(-1)^m \exp\left(-\frac{D\pi^2 m^2 t}{L^2}\right)\right] \quad (1)$$

One can see that the IDP experimental curve is perfectly described by TMAP 7, and its rising part is perfectly described by (1). Similarly good agreement was obtained also for the majority of experiments at various temperatures.

Among various regimes of IDP, this agreement can be expected in RD (or DD) regimes (see [8] for details of the regimes) if an equilibrium concentration in the implantation region establishes much faster than the characteristic time for diffusion through the membrane. The later condition is proved by the observation that the steady state re-emission [5,9] establishes much faster than the steady state permeation.

Cleaning of the virgin outlet surface by the Ar^+ beam with the flux of 10^{17} Ar/m^2 and the energy of 1.5 keV for 2 h led to the five fold increase of the permeation rate. Subsequent cleaning led to minor changes both in the permeation dynamics and the steady state permeation rate. Therefore, diffusion limited regime was supposed to be the case on the outlet side after cleaning.

In the case of DD-regime the permeation flux should be equal to

$$J = F_{\text{inc}}\left(\frac{rD_b}{LD_f}\right) \quad (2)$$

where F_{inc} – the incident ion flux without reflected particles, r – implantation depth, L – sample thickness, D_b, D_f – diffusivities in the bulk and in the implantation region, respectively. The implantation depth for 200 eV deuterons in tungsten, as calculated by SCATTER [10] equals 5 nm, while $L = 50$ μm. The calculated reflection coefficient equals 0.64. It is usually supposed that the diffusivity in the implantation region is either the same or higher than the diffusivity in the bulk. Therefore, the permeation flux in DD regime must be below $10^{-4} \times F_{\text{inc}}$. In all our experiments the permeability is above $10^{-3} \times F_{\text{inc}}$ after outlet surface cleaning. Therefore, the regime on the front side was determined as recombination limited.

So, the regime of IDP permeation was identified as RD.

The agreement of the experimental and DLR model permeation curves may indicate that the population of defects is low in the experiment and an effective diffusivity can be used. Otherwise, in the case of "strong trapping", the shape of the IDP curve would be very different [11]: the increase of the permeation rate after the lag time would be of the breakthrough type.

The effective diffusivities calculated from the experimental curves by using (1) are shown in Fig. 3. Six different samples and various fluxes were used in the experiments. One can see that the data for each experimental run can be well approximated by a linear dependence typical for the Arrhenius function. The effective diffusivities at high temperatures in experiments with various fluxes for same samples were very similar; which is typical for low trap population. It is also observed that the data differ from run to run. We attribute the difference in the experimental data to difference in the defect density from sample to sample.

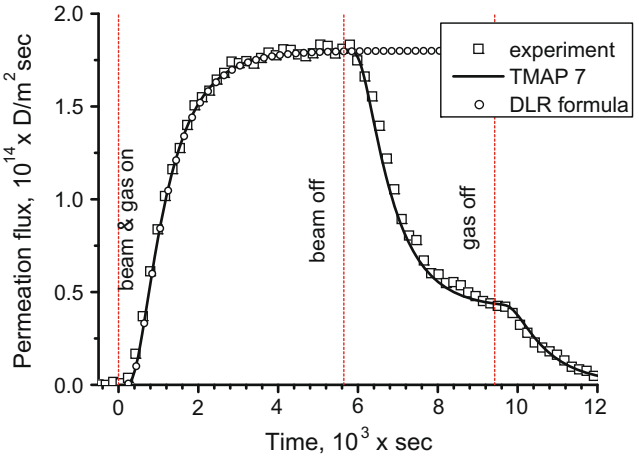

Fig. 2. Typical experimental permeation curve ($T = 893$ K, $P_{D2} = 7.7 \times 10^{-4}$ Pa, $F_{\text{inc}} = 0.36 \times 2.0 \times 10^{17}$ D/m^2) fitted using the DLR formula and the TMAP 7 code ($E_t = 2.0$ eV, $n_t = 16.5$ ppm, $K_{\text{rec}} = 3.4 \times 10^{-21}$ m^4/sec, $K_d = 2.9 \times 10^{18}$ 1/m^2/Pa).

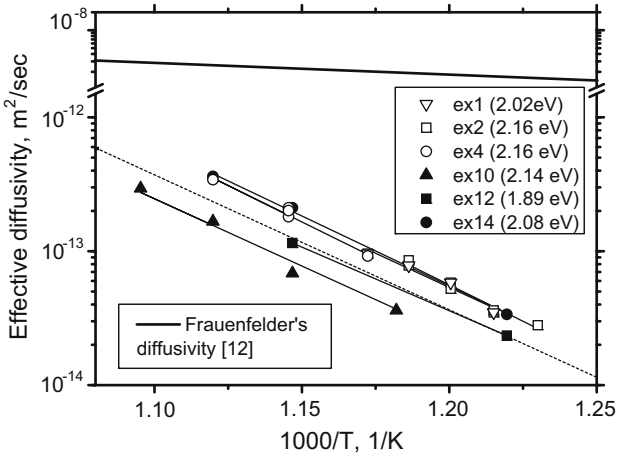

Fig. 3. Comparison of the effective diffusivities from present experiments (symbols) with Frauenfelder's approximation [10]. The specific number (see text for details) of each sample and the activation energy value for Arrhenius approximation are also shown.

All effective diffusivities in Fig. 3 are about four orders of magnitude smaller than Fraunfelder's diffusivity [12]; and this is supposed to be due to defects. The activation energy for diffusion estimated from the temperature dependence of the lag time in the experiments is (2.05 ± 0.15) eV. One must mention also the tendency of decreasing of the activation energy in the range of low temperatures.

In the case of the diffusion limited regime one can calculate the activation energy for detrapping from defects and the defect concentration. Commonly, the classic Mac-Nabb and Forster formula for the effective diffusion coefficient in the field of defects is used for this purpose

$$D_{\text{eff}} = D\left[1 + \frac{n_t}{n_a}\exp\left(\frac{E_b}{kT}\right)\right]^{-1} \quad (3)$$

where n_t and n_a are the concentrations of defects and W atoms, respectively. In the case defects retard diffusion, the second term dominates in the brackets; and the activation energy for effective diffusion D_{eff} equals the detrapping energy $E_t = E_b + E_{\text{diff}}$ (E_b – binding energy, E_{diff} –activation energy for true diffusion).

It was found in IDP experiments at high temperatures (>873 K) that GDP contribution is also important in some cases. The deuterium gas pressure on the inlet side was 7×10^{-4} Pa. Fig. 2 illustrates this conclusion. The permeation rate after the "beam off" decreases to some non-zero level that was attributed to permeation from deuterium gas. The permeation rate decreases to zero only after the "gas off". A high level of GDP was observed either in the case of the large beam spot or in the case of electrochemical polishing of the front side. One can assume that an oxide layer on the front surface suppresses GDP while ion bombardement removes the oxide layer. Therefore we take either irradiated or polished area in the case of unpolished and polished samples, respectively, for GDP calculations. Assuming that GDP takes place in DLR (clean surface), one can calculate the product of the solubility and the diffusivity $S \times D$ from the level of GDP after the "beam off". Here D is the true diffusion coefficient without defects. This gives $S \times D$ products 4–9 times higher than the Frauenfelder's value [12] for hydrogen (Fig. 4). One should mention that the gauge for the deuterium pressure measurements was situated far from the sample and the pressure could be underestimated. Therefore, these data is an upper limit and one can say that we have a good agreement of $S \times D$ product with Frauenfelder's value. The effective diffusion coefficients during IDP were several orders of magnitude smaller than the Frauenfelder's values.

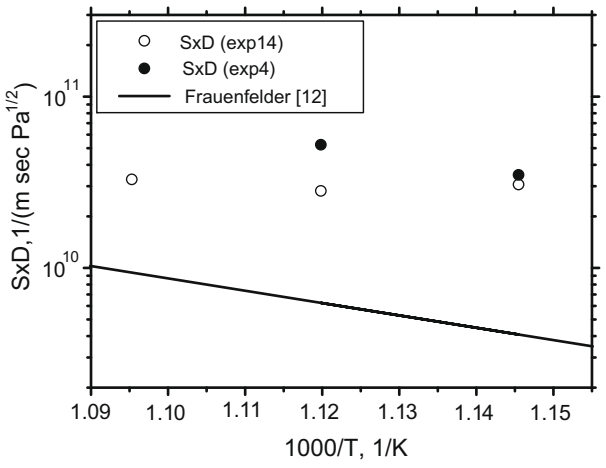

Fig. 4. Comparison of the solubility and diffusivity product from present experiments (symbols) with the corresponding Frauenfelder's value [12].

4. TMAP 7 modelling

Fig. 2 shows an example of TMAP 7 [13] calculations fitted to the experiment at 893 K. Both IDP and GDP were taken into account. The true diffusivity was taken according to Fraunfelder [12] $D(T) = 4.1 \times 10^{-7}$ exp(−0.39 eV/kT) m^2/sec. Other parameters were: the lattice parameter $\lambda = 3.16 \times 10^{-10}$ m, vibration frequency $\nu = 10^{13}$ sec^{-1}. The recombination coefficient on the back surface cleaned by the Ar^+ beam was taken high enough not to influence the calculations. The membrane areas were taken the same for GDP and IDP. The trap concentration, the recombination coefficient on the front side, and the solubility were varied. All equations for diffusion and trapping were the same as in [13].

One can see that all the three stages of the experiment were well reproduced. The parameters of defects in these calculations were $E_t = 2.0$ eV and $n_t = 15.6$ ppm. Each curve can be described by an infinite number of combinations of E_t and n_t as only the factor $n_t \times \exp(-E_t/kT)$ is important in calculations. But to fit all curves at various temperatures one must use the detrapping energy obtained from the temperature dependence of the effective diffusivity.

Anderl et al. [2] and Nakamura et al. [3] reported on traps with smaller trapping energies (1.56 eV at 60 ppm and 1.2–1.3 eV at 100 ppm). One may suggest that various defects coexist in rolled W. We have made TMAP modeling with two types of defects: 1.56 eV, 60 ppm (low energy and high concentration found by Anderl) and 2.0 eV, 16 ppm (high energy and low concentration found in our experiments). The low energy Anderl's defects had no influence in our case of high temperatures. Contrary, our defects with low concentration had no influence in conditions of Anderl's experiments at low temperature

There are still open questions. Calculations with the detrapping energy of 2.0 eV predict the trap saturation below 873 K, which might give an abrupt rise of permeation in time and a smaller lag time in comparison with predictions of the effective diffusivity approach. Nevertheless, these effects were not observed. The permeation curves were described well by (1) down to 823 K. Also, we have not observed significant deviations from the exponential dependence in Fig. 3. One can conclude that defects are not saturated even at 820 K.

The discrepancy between calculations and experiments can be caused by existence of defects more complicated than vacancies. Similar detrapping energies (1.8–2.2 eV) were reported in TDS experiments [14–16], where they were attributed to decoration of voids and pores, produced by ion implantation. We observed technological pores by FIB in our samples. According to [17], formation of vacancy clusters can be stimulated by annealing at the temperatures we used. Deuterium can be trapped on the pore surfaces as atoms and in the pore volume as gas. These features were not taken into account in modeling.

The existence of defects with a detrapping energy $E_t > 2$ eV can significantly increase the tritium inventory in tungsten at high temperatures, where defects with lower detrapping energy play no role.

5. Conclusions

Combined IDP–GDP permeation experiments in the temperature range of 823–923 K have been performed. IDP curves at high temperatures can be well fitted by a simple DLR formula for GDP. The effective diffusion coefficients D_{eff} are several orders of magnitude smaller than those given by Fraunfelder's approximation. This is supposed to be due to trapping by defects. The detrapping energy was determined to be (2.05 ± 0.15) eV.

GDP accompanies IDP at high temperatures. The product $S \times D$ has been found to be close to that given by Fraunfelder for interstitial diffusion.

TMAP 7 modeling of combined IDP and GDP gives a good overall agreement of all three stages of the experiment at high temperatures: rising permeation, decay after beam off, and final decay after gas pressure off.

Calculations with coexistence of two traps (2 eV at 16 ppm, as obtained in our experiments, and 1.56 eV at 60 ppm, as obtained in [2]) demonstrated that the low energy defects have no influence in our experimental conditions, while the high energy defects have no influence under conditions of [2]. High energy defects ($E_t > 2$ eV) will determine tritium inventory in tungsten at high temperatures.

Acknowledgements

We thank J. Dorner, M. Fußeder, and A. Weghorn for technical assistance, M. Rasinski for FIB analysis and S. Lindig for SEM analysis. The work was supported by ISTC Grant #2805, by the Impuls-und Vernetzungsfonds der Helmholtz-Gemeinschaft e.V., and by RFBR Grant #07-08-92280.

References

[1] G. Federici et al., J. Nucl. Mater. 266–269 (1999) 14.
[2] R.A. Anderl et al., Fus. Technol. 21 (1992) 745.
[3] H. Nakamura, T. Hayashi, et al., Fusion Eng. Des. 55 (2001) 513.
[4] H. Nakamura, T. Hayashi, et al., Fus. Technol. 39 (2001) 894.
[5] R.A. Anderl, D.F. Holland, G.R. Longhurst, J. Nucl. Mater. 176–177 (1990) 683.
[6] R.A. Anderl, R.J. Pawelko, et al., J. Nucl. Mater. 212–215 (1994) 1416.
[7] A.V. Golubeva et al., New ion-driven experiment PERMEX, in preparation.
[8] D.K. Brice, B.L. Doyle, J. Vac. Sci. Technol. A5 (1987) 2311.
[9] A.A. Pisarev et al., J. Nucl. Mater. 220–222 (1995) 926.
[10] V.A. Kurnaev, N.N. Trifonov, Phys. Scr. T103 (2003) 85.
[11] G.R. Longhurst, J. Nucl. Mater. 212–215 (1994) 1015.
[12] R. Frauenfelder, J. Vac. Sci. Technol. 6 (1969) 388.
[13] G.R. Longhurst, TMAP7: Tritium Migration Analysis Program, User Manual, Idaho National Laboratory, INEEL/ EXT-04-02352, 2006.
[14] A. van Veen, H.A. Filius, et al., J. Nucl. Mater. 155–157 (1988) 1113.
[15] M. Poon, A.A. Haasz, J.W. Davis, J. Nucl. Mater. 374 (2008) 390.
[16] O.V. Ogorodnikova, J. Roth, M. Mayer, J. Appl. Phys. 103 (2008) 1.
[17] H. Eleveld, A. van Veen, J. Nucl. Mater. 212–215 (1994) 1421.